Atmosphere

Volume 13 Number 1 1975

Canadian Meteorological Society
Société Météorologique du Canada

Atmosphere

Volume 13 Number 1 1975

Contents

Canadian Meteorological Society
Société Météorologique du Canada

The Green Flash and Clear Air Turbulence[1] [2]

Alistair B. Fraser
Department of Meteorology,
The Pennsylvania State University

[Manuscript received 16 December 1974; in revised form 24 April 1975]

ABSTRACT

There has long been speculation about why the green flash can be seen on one day, while on another apparently similar day it cannot. Although the green flash can be produced by a number of different refractive structures in the atmosphere, only one is of consequence when the viewing is done over the irregular terrain of most land surfaces. A combination of extensive observations and simple theory suggests that this refractive structure is formed by gravity waves which have wavelengths between about 0.2 and 2.0 kilometers. In the atmosphere such waves derive their energy from wind shear and are the same waves that are associated with clear air turbulence. This model not only explains the frequent observations of multiple green flashes, but also, by demonstrating a dependence on atmospheric dynamics, it accounts for the variability in the occurrence of the green flash on otherwise comparable days.

> "What I want to know, do you ever get to see that flash of green? People say they've seen it, the minute the sun disappears."
> "Now, it stands to reason, mister, any damn fool stares into the sun long enough, he'll end up seeing exactly what some other damn fool tells him he's going to see."
>
> (from *A Flash of Green* by John D. MacDonald)

1 Introduction

Anyone who enjoys watching the sunset will appreciate that the sun can assume some very strange shapes just before it dips below the horizon. Sometimes the edges of the sun will actually become convex, such as the example in Fig. 1 taken over Lake Winnipeg. This type of distortion is produced by strong temperature inversions. Even stranger are the little spikes that occasionally seem to grow out of the sides of the sun (Fig. 2). As you watch, the spikes appear to drift up the sides until they detach and leave an island of light floating above the top of the sun. Suddenly, all the yellow color drains away from this

[1]Paper presented at the 8th Annual Congress of the Canadian Meteorological Society, May 30, 1974, at York University, Toronto.
[2]Work supported by NSF Grant No. GA-38522.

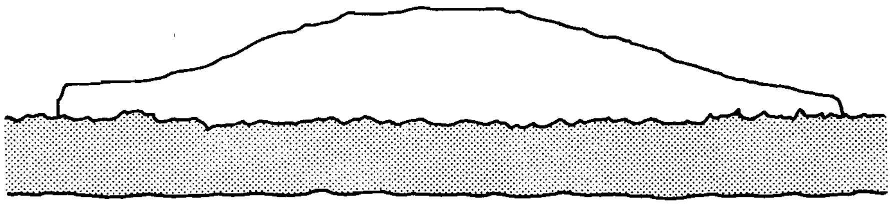

Fig. 1 This view of the setting sun was made from Grand Beach on Lake Winnipeg on August 26, 1973. The drawing was made from the projected image of a 35 mm slide that was photographed by the author. A portion of the sun, exhibiting the reverse curvature, is greatly compressed, while below that the image is greatly magnified. Such an image is seen when the temperature profile over the lake has an inflection point, that is a lifted inversion. This temperature profile is frequently found above enclosed bodies of water late in the day. The grey area below the sun is the opposite shore of the lake.

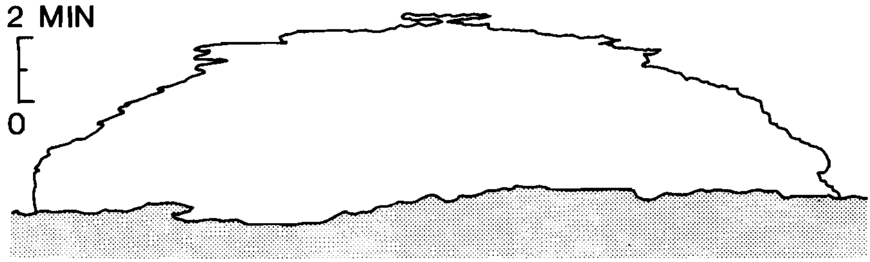

Fig. 2 This view of the setting sun was made on December 26, 1971, from Seattle, Washington, while looking out over the Olympic Mountains. The drawing was made from the projected image of a 35 mm slide photographed by the author. The grey area at the bottom is a cloud. The vertical scale shows two minutes of arc.

island and for an instant it flashes green before summarily vanishing. This is the green flash! (Actually, this represents one of four different ways the flash is manifested.)

The green flash has attracted the occasional attention of physicists ever since Jules Verne published a novel called *Le Rayon Vert* in 1882. Early interest in the phenomenon centered on the issue of "why green?". The history of this is discussed in O'Connell's book (1958). The final resolution of that problem is remarkably simple. The atmosphere is dispersive (it acts like a prism) so that the setting sun should always be seen with a red rim on the bottom and a blue rim on the top. Atmospheric scattering will usually remove the blue so that a green rim is seen on the top of the sun. Shaw (1973) discusses this aspect of the problem.

This explanation seems perfectly satisfactory (and is indeed correct) but when you calculate the angular size of the green rim under normal atmospheric conditions you discover that it is below the angular resolution of the human eye. And yet the green flash is regularly seen by naked-eye observers! There are two ways to get around this difficulty. We might ask that the green rim be magnified by the proper "mirage" conditions. One way that this can be done is the topic of much of this paper. Alternately, we could require that the main part of the sun be hidden from view, by the horizon, a mountain, or a cloud. Then if the green rim remained above the obstacle, it could be seen although it could not be resolved. (The effect is similar to viewing a star. You cannot resolve a star, but you see it because it is isolated.)

If we leave aside this rather artificial device for seeing the green rim, we are left to consider how the atmosphere can occasionally produce a short-lived magnification of a portion of the rim (the green flash generally lasts for about a second) and in particular how the phenomenon is related to the spikes that seem to extend from the sides of the sun.

2 Multiple Images

Appearances to the contrary, the spikes did not "grow" out of the sides of the sun, but are in fact multiple images of a small segment of the sun's disk. If you were to draw a vertical line through the region of these spikes (as in Fig. 4b), then each time that the line intersects the edge of a spike we are seeing another image of the same point on the edge of the sun. The spikes do not actually move up the sun, but rather, the sun as it sets moves down through the region that is producing the multiple images. The island of light that can be left temporarily "floating" above the rest of the sun is composed of two images of the upper rim of the sun. The bottom of the island is the upper rim seen inverted. As the sun moves lower in the sky, the island gets smaller and smaller until it is composed only of the two images of the green rim seen back to back. Then this vanishes as the sun gets too low in the sky to produce images in that location.

This mechanism, which produces the type of green flash that is most frequently seen over land, simultaneously doubles the angular size of the green region by combining two images and also displaces the green away from the main portion of the sun so that it is easier to distinguish. The problem of what causes this type of green flash is now reduced to the problem of what atmospheric conditions give rise to multiple images of portions of the sun.

Theorem

In a horizontally (spherically) homogeneous atmosphere it is impossible for more than one image of an extraterrestrial object (sun) to be seen above the astronomical horizon.

The mathematics of the proof of this theorem is given in Appendix I. Physically, however, if two rays of light from the same point on the sun arrive at different locations at the top of the atmosphere, then Snell's Law applied to a spherically homogeneous refracting medium requires that the two rays continue to diverge from each other as long as both rays are still passing downward through the medium (as long as the sun appears above the astronomical horizon). Thus, the two rays will not intersect anywhere to allow an eye placed at this point to see that portion of the sun at two distinct angular elevations (Fig. 3a, b).

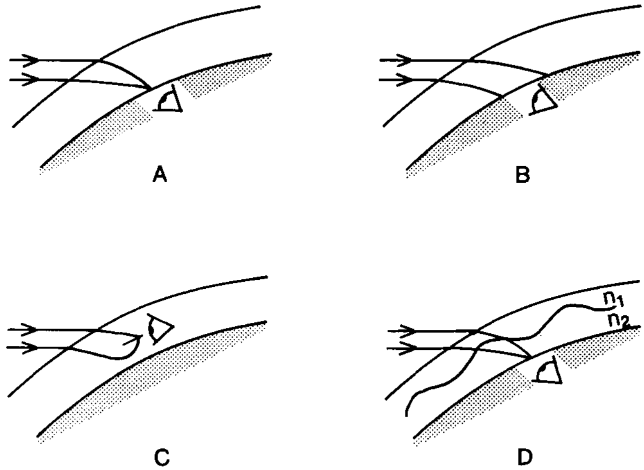

Fig. 3 Light rays that have originated from the same point on the sun pass down through the atmosphere to an observer on the earth. A. In a horizontally homogeneous atmosphere this situation is impossible. Two images of the same point cannot be seen at different elevation angles above the horizon. B. Parallel rays (originating from the same point on the sun) must always diverge as they pass down through a horizontally homogeneous atmosphere. C. Two images are possible in a horizontally homogeneous atmosphere if one image is seen below the astronomical horizon (short straight line). D. Two, or more, images can be seen above the astronomical horizon if we allow horizontal inhomogeneities such as the gravity waves on a sharp inversion surface illustrated here.

There are two ways to get around the restrictions imposed by this theorem. We could have one of the light rays (images) approach our eye from below the astronomical horizon. When this happens, we have an *inferior mirage* (Fig. 3c). The effect is identical to the second inverted image of distant automobiles and of the sky (which looks like water) that one sees when driving along a sunbaked road. When observing the sun, one generally sees the effect over oceans or large lakes when the water is warmer than the overlying air. Green flashes produced by the combination of these two images are often seen from shipboard and probably constitute the most common form of the flash seen over oceans. Under these circumstances the atmosphere can remain horizontally homogeneous.

3 Gravity Waves

The other way around the theorem is to examine an atmosphere with a horizontal inhomogeneity. Consider a stable layer which has gravity waves propagating along it. Light rays from a point on the sun that fall on a portion of the wave that is tipped towards the observer will be bent very strongly while those that fall on the portion of the wave that is tipped away from the observer will be bent weakly. It is possible in this way for both of the light rays to converge on a single location. If your eye is placed there, then two separate

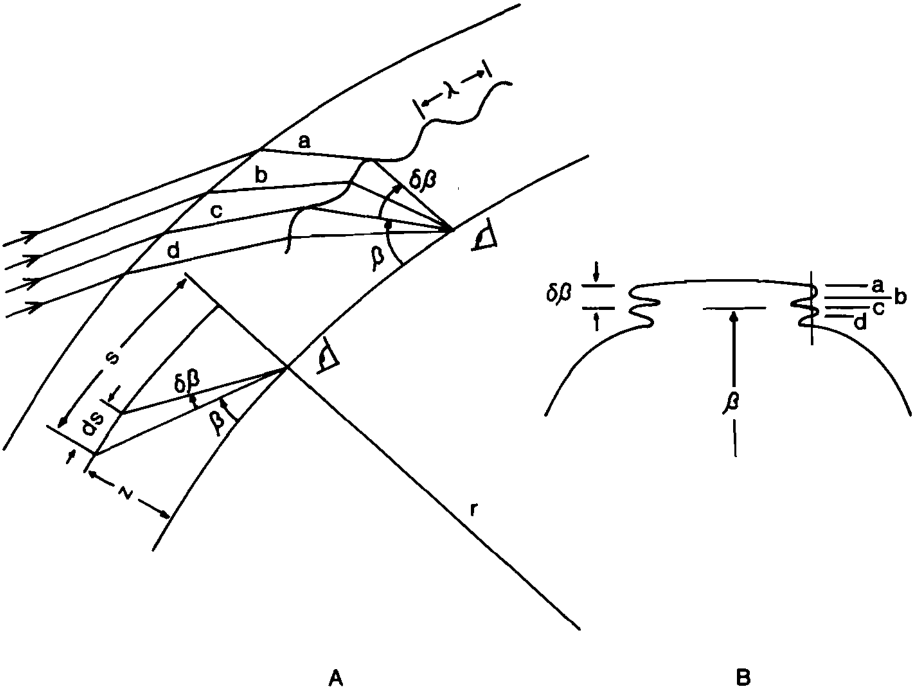

Fig. 4 A. Assume that an inversion at height z separates two layers of the atmosphere that have different refractive indices. If there is a gravity wave on this inversion surface with wavelength λ, then initially parallel rays of light a, b, c, d (coming from a single point on the sun) can all arrive at the eye. The view as seen by the eye is shown in B. The geometry of the situation is simplified on the left of A for calculative purposes (see Appendix II).

images of that point on the sun can be seen, one above the other (Fig. 3d). A more detailed analysis reveals that one of the images is always inverted. The same thing is repeated as we pass the crest of the next wave in the train.

Thus, each wavelength of the gravity waves is able to produce two images, a correct and an inverted one. We can speak of the angular wavelength of the images; the angular distance between two correct, or alternately, two inverted images. One angular wavelength corresponds to (is caused by) one space wavelength of the gravity waves so we now wish to calculate the numerical relation between the two. The question can be phrased: Are the spikes on the sun and the green flash caused by mountain waves with their characteristic scale of from 5 km to 25 km, or are they caused by billows (Kelvin–Helmholtz waves) with their characteristic scale of from about 100 m to a few km?

We will assume that there is a stable layer (inversion) in the atmosphere at height z (Fig. 4). If we are looking at an angular elevation β, then we need only calculate how far our view would shift along the inversion, ds, if we were to shift our view to $\beta + \delta\beta$. We identify $\delta\beta$ with the angular wavelength of the gravity waves. The calculation can only be performed simply if we assume that there

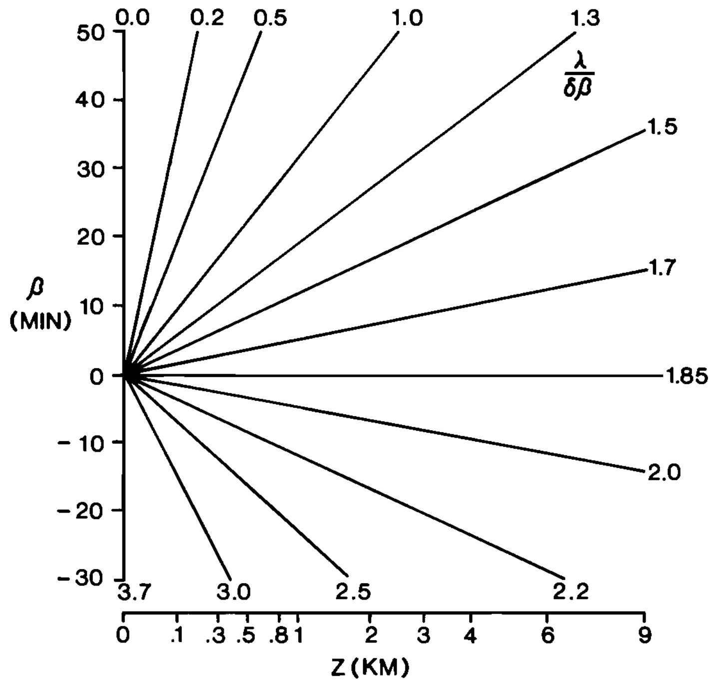

Fig. 5 The function $\lambda/\delta\beta$ is the ratio of the space wavelength λ in kilometers to the angular wavelength between similar images $\delta\beta$ in minutes of arc. The height of the inversion above the eye is z in kilometers and the angular elevation of the images above the astronomical horizon is β in minutes of arc.

is negligible refraction occurring on the ray between our eye and the inversion. As great accuracy is not required on the final answer, this is a perfectly satisfactory assumption. The mathematics of the calculation are confined to Appendix II while the results are presented in Fig. 5.

The function plotted in Fig. 5, $\lambda/\delta\beta$, is the ratio of the space wavelength, λ, in kilometers to the angular wavelength of the images, $\delta\beta$, in minutes of arc. The abscissa shows the height of the inversion in kilometers, while the ordinate shows the angular elevation of the image (above the astronomical horizon) in minutes of arc. If we consider cases where the inversion height is a kilometer or more above our eye, then it can be seen that the ratio $\lambda/\delta\beta$ has values that range between 1 and 2. This is the most significant thing that the graph shows; if the angular spacing between pairs of images is about one minute (the sun's diameter is about 32 minutes), then the multiple images are caused by gravity waves on an inversion with a wavelength of about one to two kilometers.

In both Figs. 2 and 6 the bottom of the sun was nearly touching the horizon and the multiple images were occurring near the top of the sun or at an angular elevation of about 30 minutes. In Fig. 2 the spacing between pairs of images is about a third of a minute, which would give a space wavelength of between 200 and 700 meters, depending on the assumed height of the inversion. In

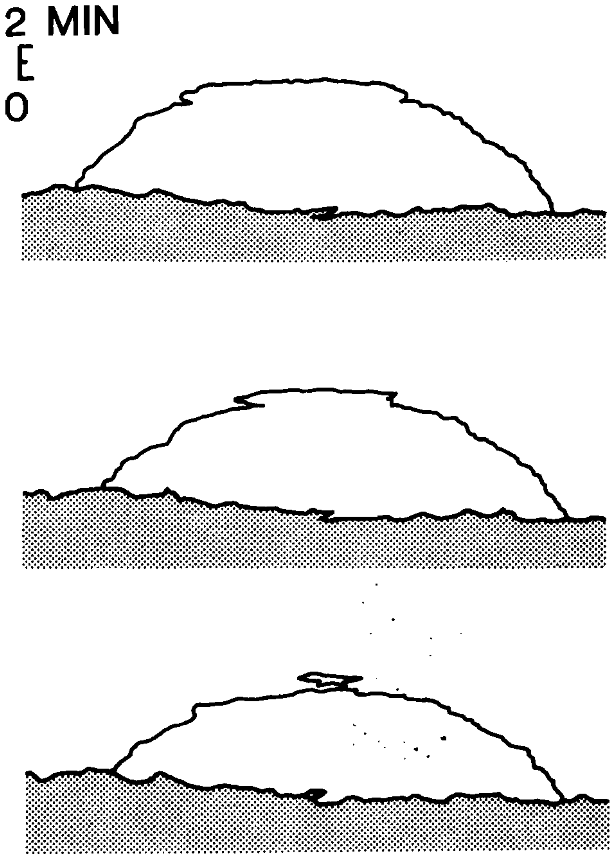

Fig. 6 This sequence (from top to bottom) of views of the setting sun was made at intervals of about three or four seconds. The drawings were made from the projected image of 35 mm slides that were taken by the author at State College, Pennsylvania, in October 1972. The scale shows two arc minutes. The sequence shows the development and appearance of the green flash when it originates with multiple images caused by gravity waves on an inversion surface. The island of light floating above the sun in the bottom picture is composed of a correct and an inverted image of the upper (green) rim of the sun. In the photograph this island is a deep green. The green lasted about a second before the island vanished. The grey area below the sun is a wave cloud formed by distant hills. The photographs discussed in this paper were taken through a catadioptric telescope (Questar).

Fig. 6 a similar calculation yields about three times those values. Extensive observing of the setting sun and its distortions indicates that these values are typical.

Because billows generally occur as a train of waves, the solar distortions often take the form of a number of spikes that move up the sides of the setting sun. It is then not unusual to see a sequence of green flashes as successive island images appear above the sun. On another apparently similar day, an observer might not see even one green flash if there were no billows present. The largest number of discrete green flashes that the author has seen during a single sunset is twenty-one and while such displays are infrequent, three or four flashes are common.

4 Conclusions

It has been shown that the spikes that sometimes extend from the sides of the sun and the green flash that is often associated with them must be caused by horizontal inhomogeneities in the atmosphere. When these inhomogeneities take the form of gravity waves propagating along an inversion layer, then observations of the angular spacing of the spikes indicate that they are generally caused by the wavelengths of between 200 m and 2 km. This is the range for shear induced gravity waves that are known to give rise to clear air turbulence. Thus we come to the somewhat surprising conclusion that the green flash, when seen above the horizon and associated with spikes on the sides of the sun, is symptomatic of clear air turbulence.

Appendix I

Theorem

In a horizontally (spherically) homogeneous atmosphere it is impossible for more than one image of an extraterrestrial object (sun) to be seen above the astronomical horizon.

Proof

Let us assume that the theorem is false and that it is possible for two parallel rays of light (coming from the same point at infinity) to impinge on the top of the atmosphere and to be refracted such that they both meet at a point (E in Figure 7). An eye at this location could thus see images at two different angles β_2' and β_1' which are both positive.

If the lower ray is labeled ray 2, then at the top of the atmosphere $\beta_2 > \beta_1$ and as we have horizontal homogeneity

$$n_t\, r_t \cos \beta_2 < n_t\, r_t \cos \beta_1$$

In a horizontally homogeneous atmosphere Snell's Law is written $nr \cos \beta =$ constant along a ray, so that it follows that

$$n_e\, r_e \cos \beta_2' < n_e\, r_e \cos \beta_1'$$

or

$$\cos \beta_2' < \cos \beta_1'$$

Now as $\beta_1' > 0$ and $\beta_2' > 0$ this requires that $\beta_1' < \beta_2'$. But as ray 2 is the lower ray, then clearly at point E, $\beta_2' < \beta_1'$ which contradicts the assumption that the theorem is false. (Strictly, we have considered only the first intersection of the rays and while on a subsequent intersection $\beta_1' < \beta_2'$ in apparent agreement with the assumption, it could not occur as the first intersection is shown to be impossible.)

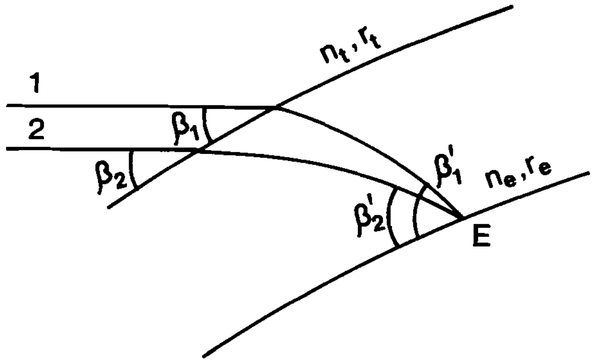

Fig. 7 These are the assumed ray paths through the atmosphere if the theorem is false. The index of refraction n, and the distances to the center of symmetry (the center of the earth) r are subscripted t (for the *t*op of the atmosphere) and e (for the *e*arth or *e*ye).

Note: Although the theorem is true in general, the proof just given breaks down when an object is located at the zenith. In this case the rays can converge on the eye but this does not give two images but rather a single very slightly magnified image. This detail is of little interest in the present context, however.

Corollary

In a horizontally homogeneous atmosphere, two images of an extra-terrestrial object are not prohibited if one image is seen below the astronomical horizon.

Proof

We have shown that $\cos \beta_2' < \cos \beta_1'$. Now if $\beta_2 < 0$ and $\beta_1 > 0$ we have no contradiction so that the rays can meet at a point.

Appendix II

Let the length of the ray traveling from the eye to the inversion be d. (See Figure 4A.) Then consider the triangle formed by the eye, the center of the earth, and the intersection of the ray and the inversion. Then,

$$(r + z)^2 = r^2 + d^2 + 2rd \cos (\beta + \pi/2) \tag{1}$$

Now β is small so $\sin \beta \approx \beta$ and $d \approx s$ and $z \ll r$ so

$$(r + z)^2 \approx r^2 + 2rz. \text{ We get}$$

$$s^2 + 2rs\beta - 2rz = 0 \tag{2}$$

Differentiation gives

$$\frac{ds}{d\beta} = \frac{-rs}{s + r\beta} \tag{3}$$

where s is eliminated to give

$$\lambda/\delta\beta = r[1 - N\ (1 + 2z/r\beta^2)^{-1/2}] \tag{4}$$

by using the expression

$$s = -r\beta + Nr\beta\ (1 + 2z/r\beta^2)^{1/2}$$

where $N = +1$ if $\beta > 0$
$N = -1$ if $\beta < 0$

and $\lambda \equiv ds$, $\delta\beta \equiv d\beta$.

Equation (4) is plotted in Fig. 5.

References

O'CONNELL, D.J.K., 1958: *The Green Flash.* North Holland Publishing Co., Amsterdam.

SHAW, GLEN E., 1973: Observations and Theoretical Reconstruction of the Green Flash. *Pure and Applied Geophysics,* **102**, 223–235.

Techniques d'Echantillonnage et d'Analyse Granulométrique des Brouillards

Michel J.E. Gauthier[1] et Conrad East[2]
Centre de Recherche en Sciences de l'Environnement
Université du Québec à Montréal[3]

[Manuscrit reçu le 19 décember 1974]

RÉSUMÉ

Dans le cadre d'une étude sur les propriétés physiques et chimiques des brouillards industriels, ainsi que sur leur potentiel nocif au point de vue biologique, on étudie les différentes méthodes d'échantillonnage et d'analyse granulométrique des brouillards, méthodes gravimétriques, optiques et par impact. Si l'on veut tenir compte de la présence des particules solides en suspension dans les gouttelettes, la seule méthode fiable est encore l'impact sur une surface amorphe qui donne un enregistrement visuel permanent.

1 Introduction

Au cours d'une recherche antérieure, East a souvent observé au-dessus de Montréal la présence d'un brouillard dans des conditions où aucun brouillard ne couvrait la région avoisinante. Ce brouillard artificiel originait des cheminées et des tours de refroidissement du vaste complexe industriel sis dans l'extrémité nord-est de l'île de Montréal. Par vents soufflant du nord-est, ce brouillard s'étendait à la grandeur de l'île de Montréal recouvrant ainsi un secteur fortement peuplé.

Comme ces brouillards surviennent assez fréquemment, spécialement au début de l'hiver, qu'ils sont probablement acides et peuvent contenir certaines substances plus ou moins toxiques, une étude fut entreprise pour en étudier les propriétés physiques et chimiques, spécialement de part et d'autre du seuil des particules respirables aux environs du diamètre de 5 μm.

Ce premier article fait rapport des techniques d'échantillonnage et d'analyse granulométrique des brouillards et du choix qui fut fait, eu égard aux objectifs. Notons que le brouillard à étudier se forme dans une atmosphère riche en particules en suspension: il faut donc utiliser une méthode qui puisse différencier entre les gouttelettes et les particules en suspension.

[1]Affiliation actuelle: Université Nationale du Rwanda, B.P. 117, Butare, Rwanda, Afrique Centrale.
[2]Auteur à qui il faut adresser toute correspondance.
[3]B.P. 8888, Montréal, Québec H3C 3P8

2 Méthodes Gravimétriques

Les méthodes gravimétriques à grand volume d'échantillonnage utilisées principalement pour les particules solides en suspension ("Hi-Vol" et impacteur Andersen, par exemple), mais aussi pour les gouttelettes de brouillard ou de nuage, consistent à récolter les gouttelettes de brouillard sur un papier filtre qu'on pèse avant et après l'échantillonnage. Avec cette méthode, il survient généralement des pertes par évaporation qui nécessitent l'analyse immédiate de l'échantillonnage. L'eau recueillie sur le filtre peut même être entraînée par l'écoulement de l'air pendant l'échantillonnage.

Par contre, si on suppose, comme l'ont fait Ludwig et Robinson (1970), que l'eau seule s'évapore et que toute substance dans les gouttelettes reste sur les filtres, on peut faire quand même une analyse de la répartition des constituants du brouillard selon le diamètre des gouttelettes. On n'obtiendra pas cependant une répartition de la quantité d'eau en fonction du diamètre.

3 Techniques photographiques

Ces méthodes consistent à photographier directement les gouttelettes de brouillard qui passent dans un volume très restreint dans le champ d'un microscope. Si on connaît le volume d'observation, on peut calculer la densité des gouttelettes. En général, cette méthode n'est applicable que pour des particules ou des gouttelettes assez grosses, bien que Phan-Cong et Dinh-Van (1973) aient réussi à mesurer par cette méthode les coefficients de coagulation de gouttelettes aussi petites que 1 μm. Mais ceci fut réalisé en laboratoire, non dans le milieu naturel.

4 Techniques optiques

Les techniques optiques consistent généralement à mesurer la lumière diffusée par une particule individuelle (gouttelette ou particule solide) qui passe devant un pinceau de lumière. L'intensité de la lumière diffusée est proportionnelle à la grosseur de la particule. Les aspects théoriques et pratiques de ces techniques ont été étudiées depuis plusieurs années avec une application presque exclusive aux particules en suspension. D'ailleurs la théorie suppose toujours qu'on a affaire à un aérosol d'une composition uniforme puisque la diffusion de la lumière dépend aussi de l'indice de réfraction des particules. La technique a cependant l'avantage de compter les particules une à une et d'observer assez facilement les particules sub-microniques d'un diamètre aussi bas que 0.1 μm.

Ces compteurs peuvent donner des résultats assez précis mais dans les conditions d'humidité relative très élevée que nous devions rencontrer, il y avait possibilité de condensation sur les parois du système optique. Pourtant, les fabricants affirment que ces appareils sont utilisés dans des chambres à brouillard (cloud chambers) sans problème. Cette technique n'est pas pratique pour nous, parce que nous voulons voir non seulement les variations dans la granulométrie des brouillards, mais aussi les concentrations de particules solides dans les gouttelettes.

Lundgren et Cooper (1969) ont étudié l'effet de l'humidité sur les méthodes de diffusion optique et concluent que la quantité de lumière diffusée par un aérosol pouvait commencer à augmenter avec l'humidité relative à un niveau aussi bas que 50% selon la fraction hygroscopique de l'aérosol. Les échantillons d'aérosols peuvent être comparés de façon plus valable s'ils sont secs ou s'ils sont séchés à une humidité relative assez basse, environ 30%. Les compteurs optiques sont affectés par l'humidité de sorte que la granulométrie de particules hygroscopiques ne sera pas la même à différentes humidités. Nous ne pouvons pas chauffer le brouillard pour résoudre le problème parce que nous voulons justement connaître la granulométrie des gouttelettes d'eau.

5 Principe des méthodes d'impact

Le nom de la méthode est bien descriptif en ce sens qu'on provoque un impact des particules de l'aérosol sur une surface qu'on observera ensuite pour voir ou bien la particule elle-même si on a pu la garder intacte ou bien une trace de l'impact. Cette trace pourrait être une tache sur un papier, une empreinte sur un film, un cratère sur une surface gélatineuse, etc. Il faut produire un étalonnage ou établir une corrélation quelconque entre les propriétés de la trace et celles de la particule qui l'a produite. Il existe une exception à cette description générale: il s'agit de la méthode gravimétrique qui est quand même une méthode d'impact, mais qui ne permet pas de compter les gouttelettes une par une.

La technologie se divise en deux parties: la conception d'un impacteur et la préparation de la surface d'impact. Ces deux parties ne sont pas indépendantes mais on peut les étudier séparément.

6 Impacteurs

Un impacteur sert à échantillonner l'aérosol et cet échantillon doit être représentatif. Les propriétés hydrodynamiques d'un aérosol varient selon le diamètre des particules et il faut prendre certaines précautions pour échantillonner aussi efficacement les petites et les grandes particules. On dit que l'échantillonnage doit être isocinétique.

On utilise souvent plusieurs étages, comme dans l'impacteur à cascades, qui récolte d'abord les plus grosses particules par des impacts à faible vitesse, puis successivement des particules plus petites à des vitesses de plus en plus grandes. Le pionnier des impacteurs à cascades est sûrement celui de May (1945).

7 Surface d'impact

On utilise différentes surfaces selon le type d'impacteur, les facilités disponibles au moment de l'échantillonnage, la possibilité de préparer les plaques d'avance, la nécessité de conserver l'échantillon et l'analyse à faire. On peut ainsi distinguer deux types d'analyses importants, l'analyse physique et l'analyse chimique, c'est-à-dire la granulométrie et l'identification des constituants, acide sulfurique, sulfates, chlorures, etc.

Dans les méthodes gravimétriques, on doit utiliser des plaques légères, pour des raisons évidentes, et inertes, spécialement si on veut faire une analyse chimique de l'échantillon. Le teflon a été utilisé pour cela et semble le meilleur matériau.

Pour faire la granulométrie d'un aérosol liquide, on utilise des surfaces visqueuses comme de la graisse ou de l'huile si on veut emprisonner les gouttelettes ou une substance amorphe, comme de la gélatine, du polyvynil ou de la lanoline, si on veut obtenir des impacts de gouttelettes. Différentes substances ont été utilisées et les plus importantes seront analysées ici. Les méthodes les plus répandues semblent utiliser la gélatine et le formvar. Les efficacités de collection de certaines méthodes apparaissent assez pauvres pour les gouttelettes de diamètre inférieur à 4 μm, où certains auteurs ont démontré une mauvaise correlation de la distribution avec la visibilité.

Plusieurs chercheurs ont analysé les propriétés de quelques surfaces d'impact pour la granulométrie des gouttelettes d'eau de nuages ou de brouillards. Rinehart (1969) a passé en revue un bon nombre de ces travaux dans le cadre d'un programme de recherches sur les brouillards des aéroports.

Dessens (1961) et Godard (1960) ont employé du collargol. Les films de collargol doivent cependant être préparés de 5 à 10 minutes avant d'être utilisés. Phan-Cong (1973) a utilisé aussi du collargol et soutient que ce milieu est plus fiable que la gélatine, en particulier parce que le facteur d'étalement est connu avec plus de précision et qu'il est indépendant du diamètre de la gouttelette. De plus, il semble que des impressions de bonne qualité puissent être obtenues sans l'usage de la microscopie en contraste de phase si on utilise des plaques de collargol fraîchement préparées.

Dans le cas de la gélatine, la surface idéale est la plus mince couche possible de gélatine pure. On peut obtenir une couche pratiquement plane. Tout colorant et vraisemblablement toute substance ajoutée à la gélatine cause des irrégularités au moment de la prise ou de la coagulation et sera donc rejeté. May (1961) et Garland (1971) ont observé la même chose surtout depuis qu'on a des microscopes plus perfectionnés.

Golitzine (1951) et plus tard Pettit (1967) ont utilisé de l'huile (type ESSO SAE 250) sur la plaque de leur impacteur. L'avantage marqué qu'ils ont retenu est que les gouttelettes de brouillard captées par l'huile conservent leur forme et leur volume assez longtemps pour pouvoir être photographiées et analysées plus tard. On mesure donc directement les dimensions des gouttelettes, mais on ne peut pas conserver l'échantillon parce que l'eau s'évapore et on doit nécessairement avoir un équipement assez élaboré, ce qui n'est pas pratique sur le terrain.

Dans notre recherche, la gélatine a été adoptée à cause des avantages suivants: préparation préalable au labo, clarté de l'impact au microscope, permanence des plaques. Avant d'être utilisées dans l'impacteur, les plaques sont systématiquement vérifiées au microscope bien qu'une technique de préparation bien soignée rend cette précaution inutile. Les plaques, une fois soumises à l'impact des gouttelettes, sont ensuite analysées au microscope.

8 Facteur d'étalement

Un avantage de la méthode d'impact des gouttelettes d'aérosol sur une surface amorphe qui a été observé par May (1945) est qu'on peut conserver l'échantillon aussi longtemps que l'on veut et qu'on n'a pas besoin de photomicroscope sur le terrain. Par contre, pour relier le diamètre de la trace au diamètre de la gouttelette, on doit connaître le facteur d'étalement des gouttelettes qui est défini comme le rapport du diamètre du cratère sur le diamètre de la gouttelette avant l'impact. Ce facteur est propre à chaque substance et dépend de la viscosité et de la densité de la gouttelette aussi bien que de la surface d'impact.

Quelques chercheurs ont tenté d'évaluer ce facteur d'étalement et les résultats sont plus ou moins concluants.

Schaefer (1962) a estimé à environ 1.25 le facteur d'étalement de gouttelettes d'eau sur du Formvar 15–9E. Okita (1968) a mesuré le facteur d'étalement de gouttelettes d'acide sulfurique sur des plaques de verre recouvertes de silicone. Les gouttelettes ont une forme hémisphérique et il existe un rapport 1.48 entre le diamètre d_s des particules sur la plaque et leur diamètre d_a dans l'air. Godard (1959) a mesuré un facteur d'étalement entre 2.2 et 2.5 pour un mélange de collargol et de gélatine dans un rapport 1 à 4.

Liddell et Wootten (1957) ont utilisé un colorant, du Vert de Naphtol B, dans de la gélatine appliquée sur les plaques d'un impacteur à cascades. L'étalonnage de la trace qui reste après l'évaporation d'une gouttelette qui a fait un impact sur la plaque montre que, en moyenne, la trace a un diamètre 2.5 fois plus grand que le diamètre de la gouttelette. La méthode peut servir pour des gouttelettes allant jusqu'à moins de 1 μm de diamètre. Ces auteurs ont utilisé comme méthode étalon, la "méthode absolue" de May (1945), méthode dont la précision a été mise en doute par Reif et Mitchell (1959) dans leur revue des méthodes d'impact.

Plus tard, Labourdique et Piekarski (1970) ont mesuré le facteur d'étalement pour la gélatine colorée et pour la lanoline colorée au Noir Soudan et obtiennent respectivement 1.6 et 1.27. May (1959) a perfectionné la méthode avec la gélatine en éliminant le colorant et en utilisant une mince couche d'environ 1 μm d'épaisseur de gélatine pure en solution aqueuse à 5%. Meszaros (1965) a obtenu une valeur de 1.4 tandis que Garland (1971) a utilité aussi de la gélatine pure mais a montré la grande supériorité du contraste interférentiel de Nomarski pour observer les cratères laissés par des gouttelettes d'eau pure. Cet auteur utilise un facteur d'étalement de 1.7. Enfin, plus récemment Kumai (1973) et Pettit (communication privée, 1973) ont utilisé un facteur d'étalement de 2.

L'analyse de Rinehart (1969) des méthodes d'impact a été faite sans l'aide du microscope à contraste interférentiel. Il conclut que la gélatine ne peut pas enregistrer d'impacts de très petites gouttelettes. Depuis que Garland (1971) a démontré la grande supériorité du contraste interférentiel sur le contraste de phase pour observer les impacts de gouttelettes, la gélatine est devenue à notre avis la surface la plus pratique. Plusieurs expérimentateurs utilisent

TABLEAU 1. Facteur d'étalement d_s/d_a de la gouttelette d'eau pour diverses surfaces d'impact. (d_s, diamètre sur la surface; d_a, diamètre dans l'air).

Auteur	Surface d'Impact	Facteur d'Etalement
Schaefer (1962)	Formvar	1.25
Godard (1959)	Collargol et gélatine	2.2–2.5
Liddell et Wooten (1959)	Gélatine colorée	2.5
Labourdique et Piekarski (1970)	Gélatine	1.6
Labourdique et Piekarski (1970)	Lanoline colorée	1.27
May (1959)	Gélatine	1.7
Garland (1971)	Gélatine	1.7
Pettit (1973)	Gélatine	2
Meszaros (1965)	Gélatine	1.4

actuellement la gélatine bien que les Français semblent préférer en général le collargol.

Le Tableau 1 résume ce qui vient d'être exposé à propos des surfaces d'impact et des facteurs d'étalement.

9 Coefficient de captation

Dessens (1961) a conçu un capteur classeur de particules à lame unique permettant un captage surveillé et dimensionné de particules. Il a étudié aussi, à l'aide d'un capteur à deux jets spécialement conçu à cet effet, le rendement de captation de ce capteur à lame unique et de l'impacteur à cascades Casella. Pour des gouttelettes de rayon entre 1 et 30 μm, il obtient un rendement qui varie entre 0.7 et 0.8 selon le rayon de la gouttelette. Toutefois le rendement diminue progressivement de 0.7 à 0.6 pour des rayons de 25 à 30 μm.

A notre avis, on devrait tenir compte de ce facteur de rendement, spécialement dans le calcul du contenu en eau du brouillard, là où les grosses gouttelettes ont une contribution très importante. Comme le soutient Dessens (1961) les coefficients de captation ne sont pas connus pour les gouttelettes de rayon inférieur au micron, car les impacteurs ne sont pas construits en vue de l'étude de particules submicroniques; l'observation sur lame de telles particules devient en effet délicate, et il est préférable de lui substituer l'observation après captation sur fils fins.

10 Granulométrie

Pour mesurer les impacts de gouttelettes et les classer par grandeur, Patterson et Cawood (1936) ont conçu un graticule. Ils ont fait la revue des méthodes utilisées antérieurement pour la granulométrie des particules de fumée et ont montré qu'aucune n'était fiable. Ils décrivent alors une méthode qui consiste à ramasser des particules de fumée sur une lame par sédimentation tel que décrit par Whytlaw-Gray *et al.* (1936) puis à examiner la lame avec un microscope muni d'un graticule dans l'oculaire. Le graticule contient un rectangle et une série de dix cercles et de dix disques numérotés. Ces derniers apparaissent en superposition dans le champ du microscope et les particules contenues dans le rectangle peuvent être rapidement comparées à l'œil avec les disques et les cercles pour obtenir leur grosseur. Environ 50 surfaces sont ainsi observées sur chaque lame et on fait la moyenne des résultats. Puisque l'aire du rectangle est connue, le nombre de particules par centimètre cube est facile à calculer. La méthode est applicable à des particules plus grandes que 0.4 μm et à des particules non hygroscopiques d'assez grand parcours moyen.

11 Conclusions

A la suite de cette revue des techniques d'échantillonnage et d'analyse granulométrique des brouillards, nous avons porté notre choix sur les techniques suivantes:

1) Méthode d'impact avec impacteur à cascades Casella;
2) Lamelles de verre recouvertes d'une mince couche de gélatine pure pour obtenir des empreintes permanentes des gouttelettes. Les lamelles, préalablement à tout usage, sont examinées au microscope, et seules celles qui offrent une surface homogène sont acceptées;
3) Adoption d'un facteur d'étalement de 2;
4) Comptage de gouttelettes au microscope à contraste interferentiel de Nomarski avec le graticule May–Porton.

Cette méthode sera utilisée dans l'étude de brouillards qui paraîtra dans un article subséquent.

References

DESSENS, J., 1961: Un capteur classeur de particules à lame unique. *Bull. Obs. Puy-de-Dome*, No. 1, 1–13.

GARLAND, J.A., 1971: Some fog droplet size distributions obtained by an impaction method. *Quart. J. Roy. Meteorol. Soc.*, **97**, 483–494.

GODARD, L., 1959: Procédé pour déterminer les dimensions des gouttelettes de brouillard ou de nuages. *Bull. Obs. Puy-de-Dome*, No. 1, 11–13.

GODARD, S., 1960: Mesure des gouttelettes de nuage avec un film de collargol. *Bull. Obs. Puy-de-Dome*, No. 2, 43–46.

GOLITZINE, N., 1951: Method for measuring the size of water droplets in clouds, fogs and sprays. National Aeronautical Establishment, Note 6 (ME–177), Ottawa.

KUMAI, M., 1973: Arctic fog droplet size distribution and its effect on light attenuation. *J. Atmos. Sci.*, **30**, 635–643.

LABOURDIQUE, D. et PIEKARSKI, S., 1970: Etude d'une méthode de captation de petites gouttes d'eau et mesure de leur diamètre. *J. Rech. Atmos.*, 129–138.

LIDDELL, H.F. et WOOTTEN, N.W., 1957: The detection and measurements of water droplets. *Quart. J. Roy. Meteorol. Soc.*, **83**, 263–368.

LUDWIG, F.L. et ROBINSON, E., 1970: Observations of aerosols and droplets in California stratus. *Tellus*, **22**, 94–105.

LUNDGREN, D.A. et COOPER, D.W., 1969: Effect of humidity on light-scattering methods of measuring particle concentration. *J. Air Poll. Control. Assoc.*, **19**, 243–247.

MAY, K.R., 1945: The cascade impactor: an instrument for sampling coarse aerosols. *J. Sci. Instruments*, **22**, 187–195.

MAY, K.R., 1959: Detecting volatile airborne droplets. *Nature (London)*, **183**, 742–743.

MAY, K.R., 1961: Fog-droplet sampling using a modified impactor technique. *Quart. J. Roy. Meteorol. Soc.*, **87**, 535–548.

MESZAROS, A., 1965: Concentration et distribution dimensionnelle des gouttelettes de brouillards atmosphériques. *J. Rech. Atmos.*, No. 9, 53–64.

OKITA, T., 1968: Concentration of sulfate and other inorganic materials in fog and cloud water and in aerosol. *J. Meteorol. Soc. Japan*, **46**, 120–127.

PATTERSON, H.S. et CAWOOD, W., 1936: The determination of size distribution in smokes. *Trans. Faraday Soc.*, **32**, 1084–1088.

PETTIT, D.G., 1967: Airborne Instrumentation for a Cloud Physics Research Project. National Research Council of Canada, Aeronautical Report LR–490, Ottawa.

PHAN-CONG et DINH-VAN, P., 1973: Direct measurement of coalescence efficiency and frequency of small water droplets in an electric field. *Tellus*, **25**, 63–68.

REIF, A.E. et MITCHELL, C., 1959: Size analysis of water aerosols. *Ann. Allergy*, **17**, 157–172.

RINEHART, G.S., 1969: Fog drop size distributions – Measurement methods and evaluation. Atmospheric Sciences Lab., White Sands Missile Range, New Mexico, Rep. No. ECOM-5247.

SCHAEFER, V.J., 1962: The vapor method for making replicas of liquid and solid aerosols. *J. Appl. Meteorol.*, **1**, 413–418.

WHYTLAW-GRAY, R., CAWOOD, W. et PATTERSON, H.S., 1936: A sedimentation method of finding the number of particles in smokes. *Trans. Faraday Soc.*, **32**, 1055.

A Note on Fluctuations in the Normal Temperature Trend at Selected Canadian Stations

G.S. Strong[1] and M.L. Khandekar[2]
Department of Geography,
The University of Alberta,
Edmonton, Alberta

[Manuscript received 7 January 1974; in revised form 19 February 1975]

ABSTRACT

Spurious fluctuations in the normal mean daily temperatures for ten Canadian stations are filtered out, using weighted running means. The filtered curves reveal cycles of temperature peaks at intervals of about 17 days. An attempt is made to relate these cycles to the index cycles of the atmospheric general circulation.

1 Introduction

The term "January thaw" is often heard during early winter in various parts of Canada. The term refers to a short "warm weather" period that generally occurs during or around middle January in many parts of Canada. According to our recollections, two such "warm spells" were experienced during January 1968 and 1969 in Montreal and Toronto, and recent ones in Edmonton during January 1973 and 1974. In each of these four cases, the warming trend occurred just prior to the annual minimum temperature which generally occurs in late January.

In this note, long-term averages of mean daily temperatures at selected Canadian stations are closely examined. It is found that this temperature fluctuation is not only confined to a mid-January thaw, but appears over the winter months (December to March) in a quasi-periodic manner with a period of about half a month. These quasi-periodic fluctuations are especially well-marked when the raw data is smoothed out, using a scheme of running means as discussed in the next section. An attempt is made to relate these cyclic fluctuations in the mean daily temperatures to the index cycles of the general circulation.

2 Treatment of Data

Since the main objective was to study January temperatures, only the winter months of December to March are investigated here, as temperature changes are most pronounced during these winter months at mid-latitudes. Fig. 1 shows long term (more than 90 years) averages of daily temperatures for Edmonton,

[1]present affiliation: Maritimes Weather Office, Box 5000, Bedford, Nova Scotia.
[2]present affiliation: Caribbean Meteorological Inst., Box 130, Bridgetown, Barbados.

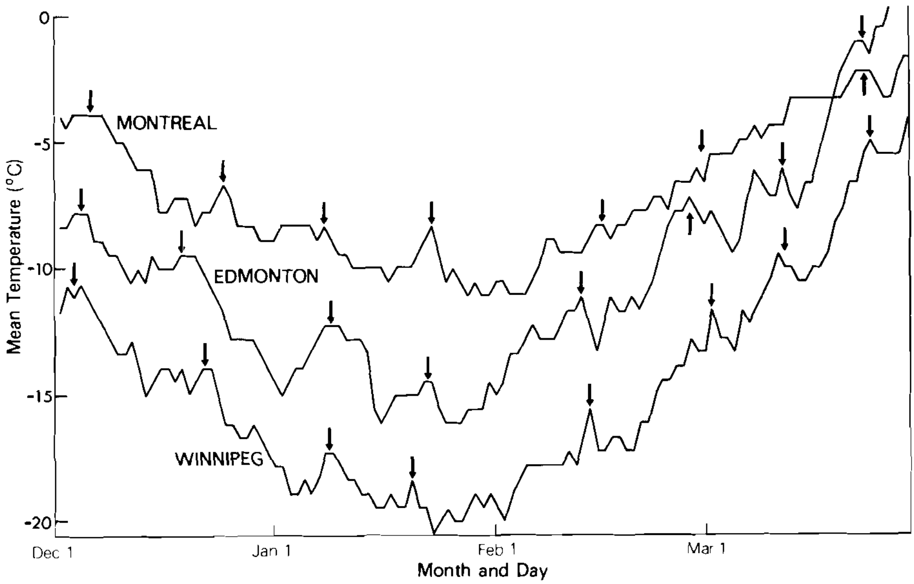

Fig. 1 90-, 98-, and 99-year averages of mean daily temperatures for Edmonton, Winnipeg, and Montreal respectively, for December 1 to March 31st. Arrows indicate the main peaks.

Winnipeg and Montreal, respectively. It can be seen that spurious fluctuations are not all filtered out by simple averaging over 90 years or more. In addition, one notes almost coincidental peaks (indicated by arrows in Fig. 1) spaced approximately half a month apart, but with some longitudinal lag in time from west to east.

In order to smooth the spurious fluctuations in the data a suitable scheme of weighted running means was used. Typically a weighted running means can be expressed as

$$\overline{T}_t = \sum_{k=-n}^{n} w_k T_{t+k}$$

$$= w_{-n}T_{t-n} + w_{-n+1}\, T_{t-n+1} + \dots w_0 T_t + \dots + w_n T_{t+n} \qquad (1)$$

Here T_t is the raw value of the temperature at time t. $\overline{T}_t$ is the corresponding smoothed value and w_n are a set of approximately chosen weights. The value of n will depend upon the length of the time over which the running mean is desired. For example, a seven-day running mean will be accomplished by choosing $n = 3$. The spurious fluctuations in our temperature records correspond to high frequency waves which can be suppressed by using a suitable scheme of running means corresponding to a low-pass filter (see Holloway, 1959). In this study, we have used a nine-day running mean having weights w, decreasing in magnitude outward from the principal weight. As pointed out by Holloway (1959), such a scheme of weighting function reduces the negative response and does not generate any unwanted ripples on the smoothed output.

The values of the weighting functions and the corresponding filter responses have been discussed by Danielson and Bleck (1970).

3 Results and discussion

Fig. 2 shows the smoothed temperature curves for Edmonton, Winnipeg, and Montreal, using 90 years or more of data. The main peaks at 15–20 day intervals stand out very clearly. Fig. 3 depicts the curve for Regina[1] which shows similar quasi-periodic fluctuations. The smoothed temperature curves for Halifax[1] and St. John's[1] (Newfoundland) are shown in Fig. 4. Since the normal temperature range for these maritime stations is relatively smaller, Fig. 4 is drawn with a stretched temperature scale; nevertheless it is interesting to note that these curves also exhibit small but definite temperature fluctuations. The smoothed curves for the remaining stations,[1] not shown here, all show essentially similar fluctuations, including Calgary[1] with its notorious chinooks throughout the winter months.

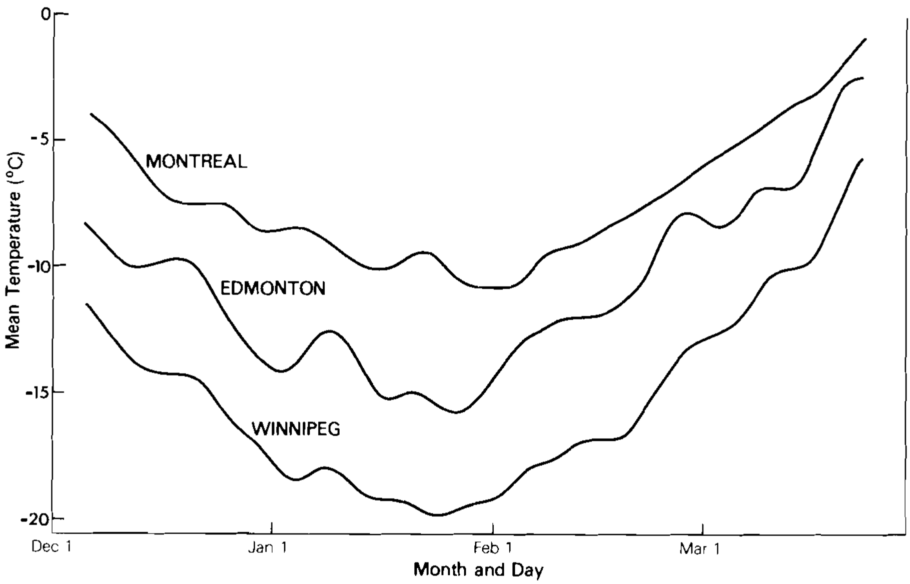

Fig. 2 Seven-day weighted running means of the 90-year(+) mean daily temperatures for Edmonton, Winnipeg, and Montreal, for December 4 to March 28.

Table 1 lists and summarizes the average period of the temperature cycle for all stations using a nine-day running mean. Here the period is defined as the average number of days between successive maxima on the filtered curves. Thus, when spurious fluctuations are filtered out, the average periods range from 15 to 20 days, giving a mean over all the stations of 17.2 days. The peaks for the smoothed curves as well as for the raw data do not coincide for all the stations; rather, there appears to be a west to east propagation of the cycle with time as can be seen from an inspection of Figs. 1 to 3.

[1]Thirty years of raw data were used for these curves.

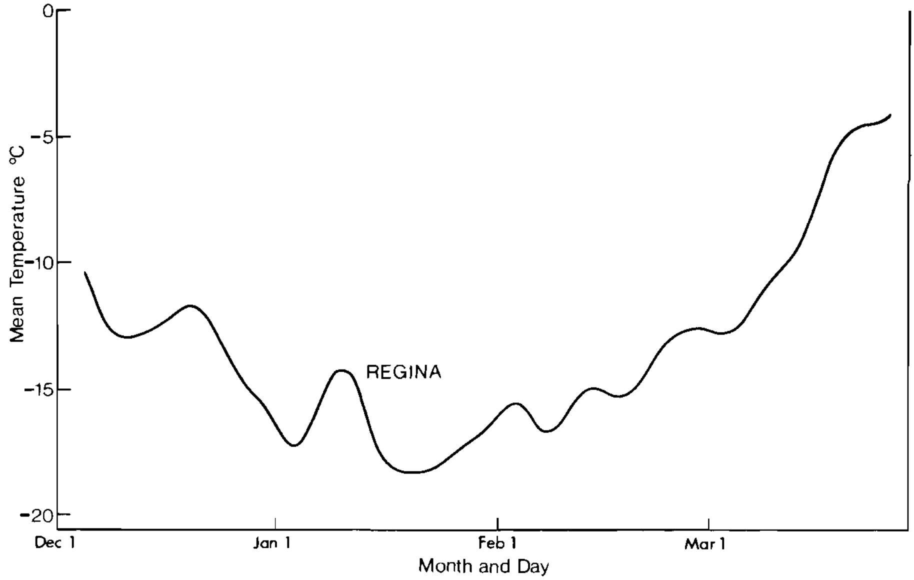

Fig. 3 Nine-day weighted running means of the 30-year mean daily temperatures for Regina, for December 4 to March 28.

The results presented above suggest a general quasi-periodic pattern of fluctuations in the normal temperatures over various parts of Canada. Similar fluctuations in the normal temperature records at selected locations in the northeastern United States have been documented by Wahl (1952) in his studies on the January thaw in New England. According to Wahl the January thaw at Boston is only a part of a much larger phenomenon, namely a change-over from a westerly circulation pattern to a northwesterly flow pattern. Such large-scale circulation patterns have been extensively studied by Namias (1950, 1953) who has attempted to relate these changes to index cycles of the general circulation. The fundamental role of the index cycles is to transport the excess of heat energy from tropical latitudes to mid-latitudes. This heat transport is accomplished through large-scale eddies, which impose quasi-periodic fluctuations on the zonal index, resulting in index cycles having periodicity from 3 to 8 weeks (see Namias, 1953). As pointed out by Namias, one also finds fluctuations of shorter periods in the index cycles, similar to the temperature fluctuations under discussion. Fig. 5, after Namias (1953), shows zonal indices at 700 mb for 5-day means for November through March for nine years. If one observes all the peaks of zonal indices for December through March, the nine-year average number of index maxima then yields a period of slightly more than 15 days, as opposed to 16–17 days for the temperature fluctuations. A comparison of Fig. 5 with Figs. 1 and 2 shows that high zonal index is in general associated with temperature peaks in raw as well as smooth data (Figs. 1 and 2). Similar results have been reported by others (see Chang, 1972).

To what latitudes do the temperature fluctuations extend? A partial answer to this can be given: Longley (1958), in his studies on temperature fluctuations

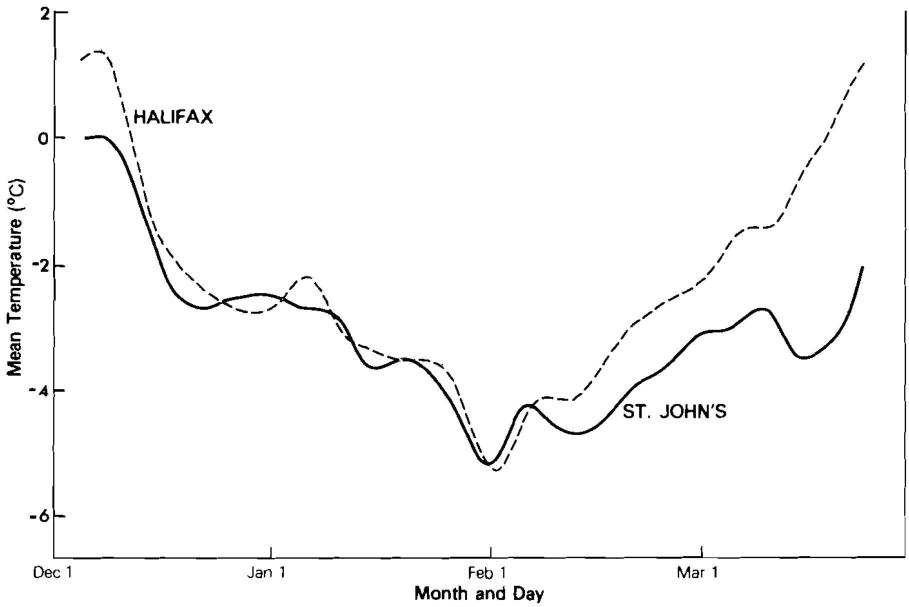

Fig. 4 Nine-day weighted running means of the 30-year mean daily temperatures for Halifax, and the 25-year mean daily temperatures for St. John's, for December 4 to March 28 (temperature scale stretched).

TABLE 1. Average Period of Temperature Fluctuations, December to March, for selected Canadian Stations.

Station	Period of Averaged Temperatures (yrs)	Period of Weighted Running Mean (days)	Average Period of Fluctuation (days)
Edmonton	90 (1880–1969)	7	15.0
Winnipeg	98 (1872–1969)	7	16.8
Montreal	99 (1871–1970)	7	17.4
	Mean of 90-year(+) data	....	16.4 days
	Median of 90-year(+) data	....	16.8 days
Edmonton	30 (1941–1970)	9	16.6
Calgary	30 (1931–1960)	9	17.8
Grande Prairie	25 (1942–1967)	9	17.2
Whitehorse	30 (1942–1971)	9	16.0
Saskatoon	29 (1942–1970)	9	19.7
Regina	30 (1931–1960)	9	17.0
Winnipeg	30 (1931–1960)	9	16.6
Montreal	30 (1941–1970)	9	15.4
Halifax	30 (1931–1960)	9	18.3
St. John's	25 (1942–1966)	9	17.0
	Mean of 25–30-year data	....	17.2 days
	Median of 25–30-year data	....	16.9 days

at Resolute, Northwest Territories, computed seven-day running means for eight years of data. Fluctuations similar to those under discussion can be observed in his smoothed data with an average period of 16 days; this is again in good agreement with the average value of the period in Table 1. No attempt

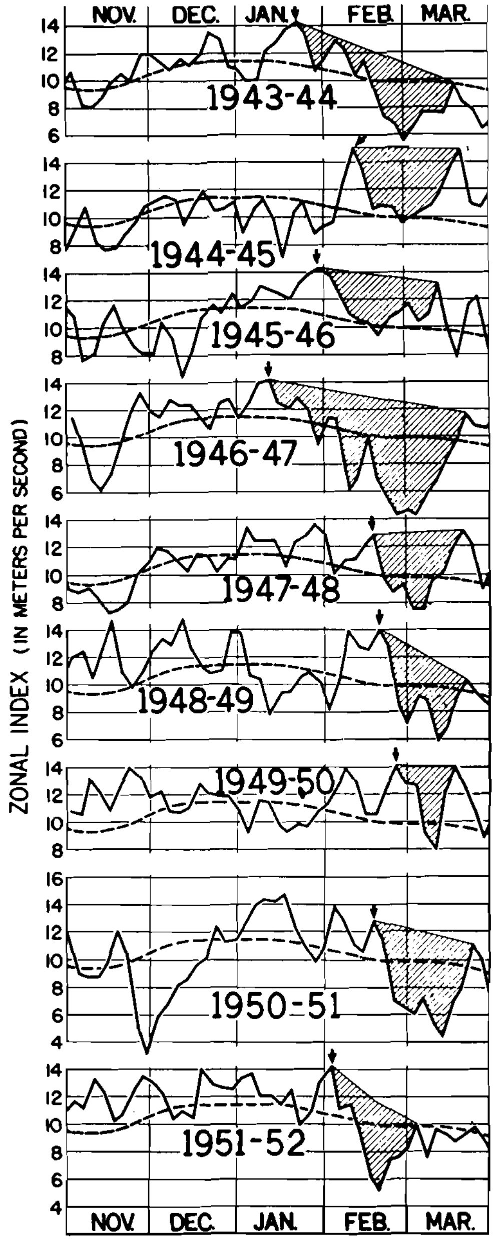

Fig. 5 Zonal indices at 700 mb for 5-day means for November through March of nine years; broken lines connect normal values for calendar months; hatched areas denote primary index cycles beginning with the high index periods indicated by arrows. After Namias (1953).

is made in this study to determine the southern extent of these temperature fluctuations.

4 Concluding remarks

The existence of a "January thaw" in the long-term records of selected Canadian stations appears to be a real feature, which is associated with the quasi-periodic temperature fluctuations having an average period of about two weeks. The general interest in a January thaw, but not in the other peaks and lulls in the annual temperature trend, is possibly due to a psychological reaction to warmer temperatures just preceding the annual minimum temperature. For example, the pronounced "cooling" in mid-February is not noted as well, perhaps because temperatures are then on the upswing anyway.

Our analysis brings out a possible relationship between the temperature fluctuations and the index cycles of the general circulation; this is in general agreement with earlier studies. As the meridional transport of heat energy is accomplished through variations of the zonal index, it appears to impose temperature fluctuations characteristic of the quasi-periodic nature of the index cycles.

It is interesting to note that these fluctuations stand out even after averaging and smoothing the temperature data for over 90 years. This seems to suggest that there may be some preferred positions (in time) for these cycles. To the best of our knowledge, none of the theoretical and observational studies on index cycles suggests any coupling between the index cycles and the time of the year. We are therefore inclined to surmise that the fixed topographic features of the earth, together with the fixed ocean-land distribution tend to induce fluctuations in the general circulation at certain preferred times of the year, excepting for minor variations. These minor but significant variations tend to make the index-cycles quasi-periodic, and hence, unpredictable.

Acknowledgements

The computing facilities provided by the University of Alberta are gratefully acknowledged. Thanks are due Mrs. Laura Smith for typing the manuscript.

References

CHANG, JEN-HU, 1972: *Atmospheric circulation systems and climates*, The Oriental Publishing Company, Honolulu, Hawaii, 328 pp.

DANIELSEN, E.F. and R. BLECK, 1970: Tropospheric and stratospheric ducting of stationary mountain lee waves. *J. Atmos. Sci.*, **27**, 758–772.

HOLLOWAY, J.L., 1958: Smoothing and filtering of time series and space fields. *Advances in Geophysics*, **4**, 351–389.

LONGLEY, R.W., 1958: Temperature variations at Resolute, Northwest Territories. *Quarterly J. Roy. Meteor. Soc.*, **84**, 459–463.

NAMIAS, J., 1950: The index cycle and its role in the general circulation. *J. Meteorology*, **7**, 130–139.

NAMIAS, J., 1953: *Thirty-day forecasting: A review of a ten-year experiment*. Meteorological Monographs, Amer. Meteor. Soc. **2**, No. 6, 83 pp.

WAHL, E.W., 1952: The January thaw in New England (An example of a weather singularity). *Bull. Amer. Meteor. Soc.*, **33**, 380–386.

The Relationship between Forest Fire Occurrence and 500 mb Longwave Ridging

M.J. Newark
Toronto Weather Office
Atmospheric Environment Service

[Manuscript received 3 February 1975; in revised form 10 April 1975]

ABSTRACT

In general terms the probability of forest fires is increased by weather conditions that:

(a) maximize the drying of forest fuels,
(b) give a minimum of rain and yet still allow enough convective activity to produce lightning and spread going fires.

The hot sunshine and dry weather of summer high pressure systems fulfill these conditions. At the earth's surface however high pressure is transitory while at the 500 millibar level, ridging is much more persistent. Such longwave ridges aloft may persist for as long as 80 days or even more but show oscillations in their strength. For the severe forest fire season of 1974 in northwestern Ontario, the changes in amplitude of the persistent longwave ridge over the area were examined. Using a diagnostic Hovmöller diagram, periodic oscillations of eleven days were discovered in its intensity which agreed closely with the periodicity in the Fire Weather Index, a measure of the forest's potential for fires. If such longwave behaviour is predictable then long term general statements about forest fire occurrence can be made.

1 Introduction

During the 1974 forest fire season 1,591 fires were recorded in Ontario with 1,288,170 acres burned. This season qualifies as one of the worst on record if only fire number and acreage are considered. The section of the province suffering the most was the area bordering on Manitoba. The greatest majority of fires in fact occurred in the Ontario Ministry of Natural Resources' northwestern fire region (fig. 1). A protracted dry spell which persisted from early June until the middle of August resulted in high to extreme values of Fire Weather Index (FWI) throughout much of the period. An emergency situation arose on July 7th and 1,700 people were evacuated from Vermilion Bay. Around the second week in August, nature took a hand and frequent rainfalls finished off the job that the firefighters had struggled with for nearly seven weeks.

It has been known for some time that longwave ridging at the 500 mb level over a particular longitudinal zone spells trouble for the firefighters in that

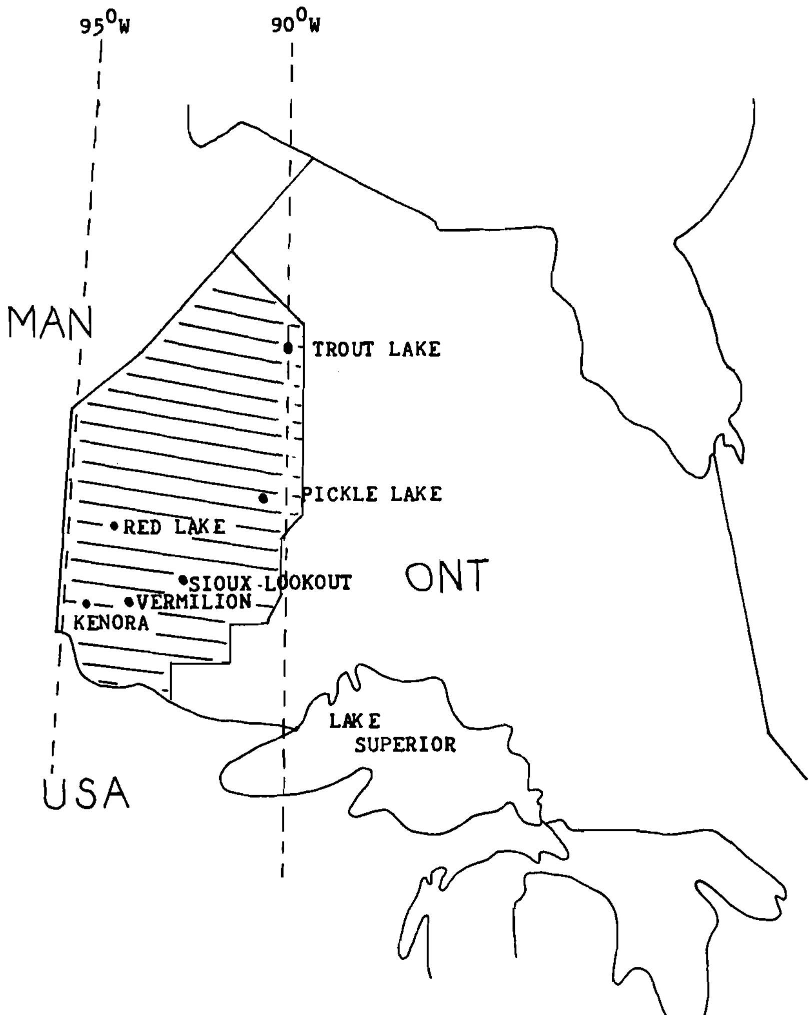

Fig. 1 The Northwest Fire Region of the Ontario Ministry of Natural Resources.

area. In order to determine what kind of relationship exists between the occurrence of forest fires and longwave ridges, an analysis was made of the 1974 season.

The first discovery was that a longwave ridge persisted at approximately the longitude of northwestern Ontario from June 14th, to August 8th, during which time the most hazardous fire weather situation of the summer occurred. Secondly, the ridge exhibited an orderly oscillating behaviour. It is possible that this is a feature of other bad fire years and that case studies will not only reveal the key to the inception of the longwave ridge but will do so in time to use the periodicity as a forecasting tool.

2 Surface weather systems

From June 14th to August 8th, high pressure systems were the dominating feature on the surface weather map. They were interspersed with occasional outbreaks of fresh dry Maritime Polar or modified Maritime Arctic air. As the northwestern fire region was dominated by a longwave ridge pattern at mid levels of the atmosphere, the troughs associated with the leading edge of the outbreaks weakened as they moved eastwards from the Rockies. This meant that rainfall was sparse and almost exclusively the result of localized convective activity. In many cases, the precipitation was associated with lightning. With the air masses being very dry, the rain in some cases would evaporate before reaching the ground leaving "dry" lightning. New fire starts were naturally the result.

3 Upper air patterns

a *The 1974 pattern*

Early in the month of June a well developed omega blocking pattern formed in the airflow at middle levels of the atmosphere over North America. By the middle of the month the western arm of this pattern had moved to Quebec followed by a mid-continent ridge. This ridge-trough configuration then persisted as a stationary longwave feature until nearly the second week of August. Most importantly, the longwave ridge remained over the northwestern fire region.

The most interesting feature of this pattern is the periodicity with which troughs broke through the ridge. The cycle typically consisted of a slow building of the ridge with associated high pressure influence at the surface, followed by a fairly rapid collapse as the troughs penetrated.

b *500 mb heights over International Falls as a longwave indicator*

A smoothed curve of the 500 mb height at International Falls versus time clearly shows the periodic building and collapse of the ridge (fig. 2). The period from ridge to ridge averaged eleven days. However, the average period from trough to trough was fifteen days so that after five cycles the pattern broke down.

c *Maximum temperatures as a longwave indicator*

To reinforce the evidence for periodicity, a check was made on the maximum observed surface temperature within the region. Since this temperature is linked to 500 mb heights, by way of the layer thickness concept, it should also show some periodic variation. In addition, it is reasonable to expect that maximum temperatures will be lower during the unsettled weather of troughs and at a peak during times of fire weather associated with ridges. A smoothed curve of the maximum temperature observed anywhere in the region in fact follows the variation of heights very closely (fig. 2).

d *Hovmöller diagram as a longwave indicator*

The Hovmöller diagram (fig. 3) very clearly shows the persistence of the

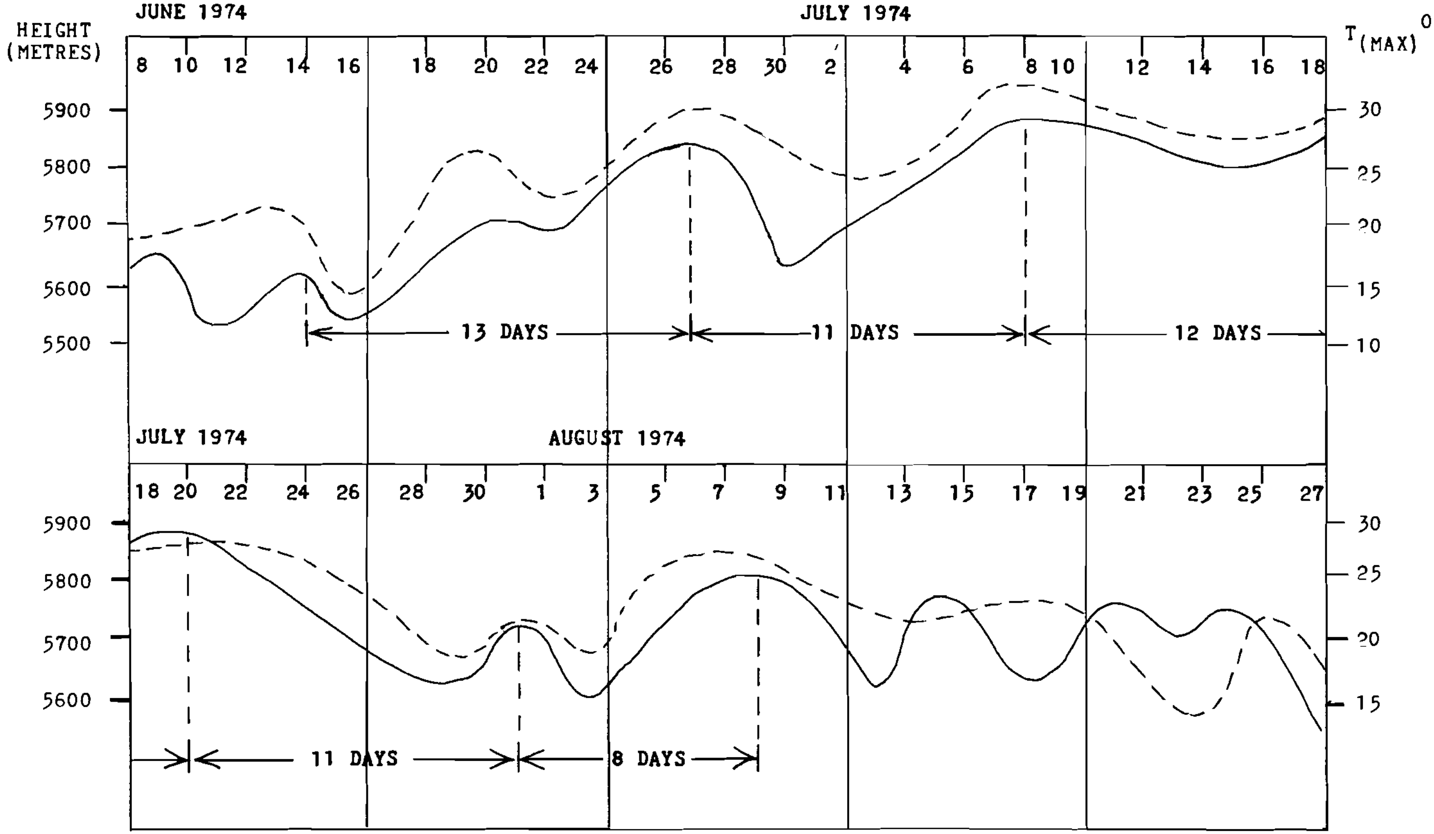

Fig. 2 Smoothed curve of 500 mb heights over International Falls compared to the smoothed curve of maximum observed temperature in the region (dashed curve). The period of each oscillation is shown in days.

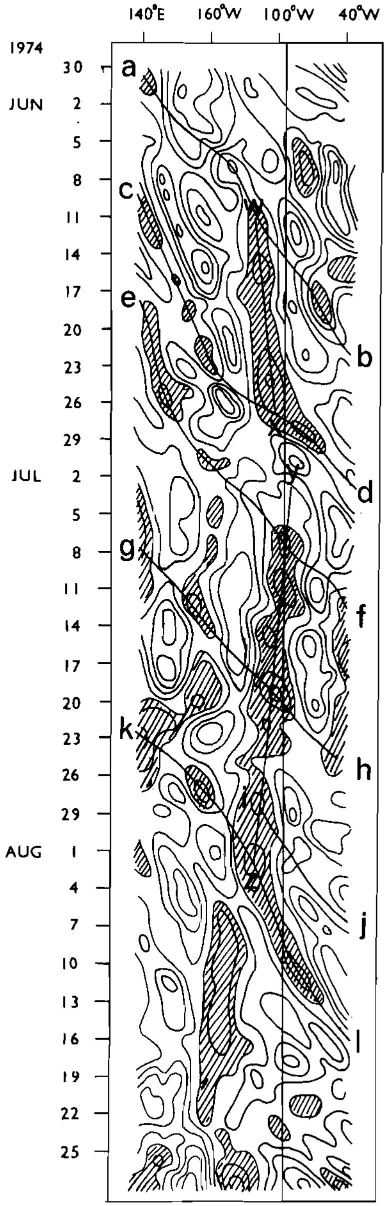

Fig. 3 Hovmöller diagram for 30th May to August 28th 1974. The unlabelled vertical line is the longitude (93°W) of the Northwestern Region. Shaded areas are ridges at 500 mb. Unshaded areas are troughs.

longwave ridge WXYZ at about the longitude of northwestern Ontario (denoted by the unlabelled vertical line at 93°W). It makes its appearance during the first week in June and persists until August 23rd. For part of this

TABLE 1. Dates that major 500 mb ridges crossed 93°W

Date of 93°W Longitude Crossing	Major Ridge Identification (Fig. 3)	Average Speed of Ridge (knots)
June 14th	A,B	11
June 27th	C,D	18
July 7th	E,F	16
July 20th	G,H	18
July 31st	I,J	12
August 8th	K,L	10

time it showed a steady retrogression of 0.83 degrees longitude per day (1.3 knots).

It is of interest to note that the wavelength of the longwave features of the circulation is approximately 65 degrees of longitude (wave number of about 6). The ridge crossed the 93°W longitude line on July 8th, just the time of the Vermilion Bay emergency! About August 5th, a particularly vigorous trough moved through the ridge destroying the comparatively stable pattern. Travelling waves then predominated at 93°W.

Throughout the lifetime of the ridge a series of major ridges and troughs moved through it. The passage of these groups across 93°W resulted in the periodicity in the fluctuation of heights at that longitude that has already been examined in fig. 2. The Hovmöller diagram (fig. 3) shows that major ridges crossed 93°W at times which are shown in table 1.

It should be noted that the peak of July 31st in fig. 2 appears as only a weak ridge in fig. 3. Apart from this, excellent agreement exists between table 1 and the times of the peaks shown in fig. 2.

The literature records several cases of periodicity in oscillations of the zonal index (Panofsky and Wolff 1957, Monin 1963, Julian 1966, Noar 1973). In this analysis, the eleven day period of oscillation relates directly to the change in amplitude of the real weather feature rather than to an index, but the similarity to the 12 to 13 day figure common in the literature suggests that they are related.

4 Fire Weather Index

The Fire Weather Index (FWI) is a numerical rating of potential fire intensity in a standard fuel type. By definition it is dependent on weather only, not on differences in fuels or topography. It is related to the ease of ignition of wild fires. The FWI combines the meteorological parameters upon which forest fires depend and forest fuel moisture content as well as a term to take account of the rate of spread of fire. The numerical value of the index is directly proportional to the potential fire intensity. In practice, various ranges of values are grouped into four fire-danger categories, namely "low", "moderate", "high" and "extreme".

Since the FWI is highly dependent on atmospheric temperature and rainfall it is reasonable to expect that its variations are somehow linked to 500 mb ridging.

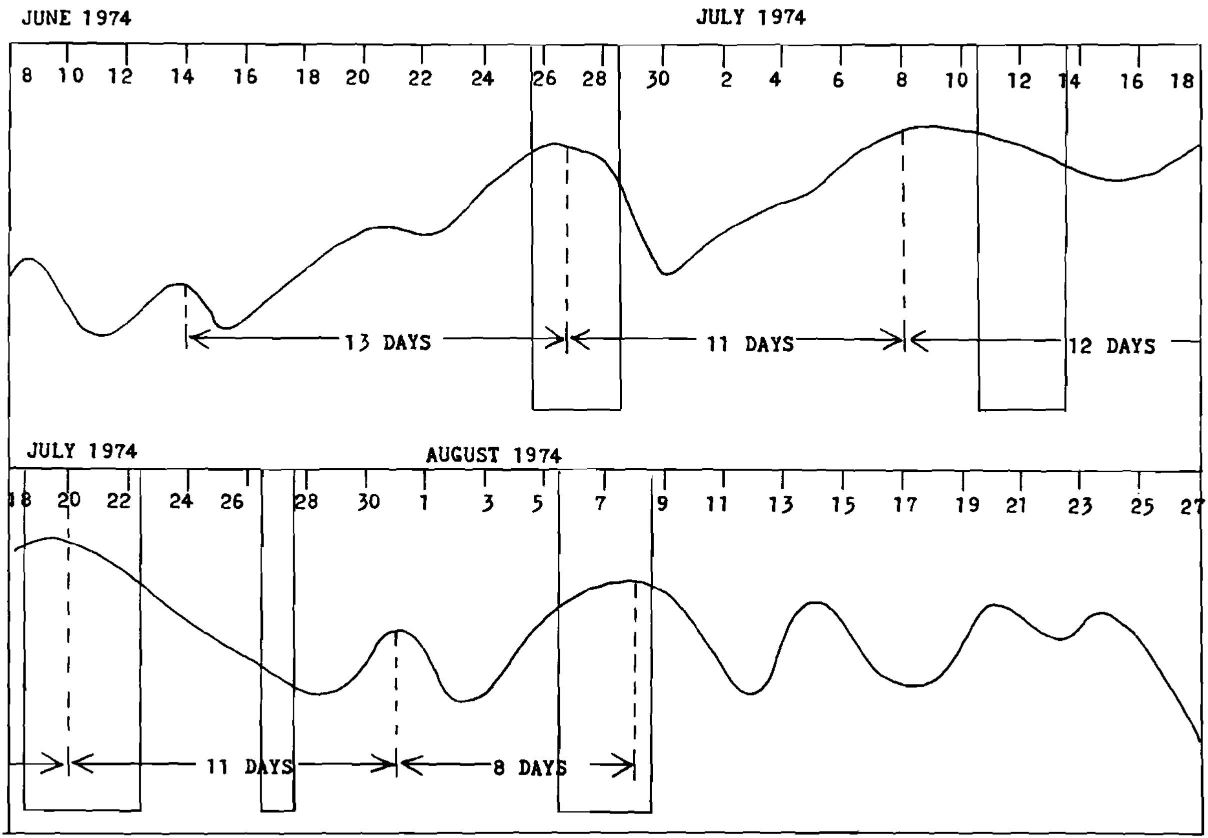

Fig. 4 Relationship between times of peak ridging (curve) and times of maximum fire weather index (rectangles).

In fact it shows an interesting and predictable relationship to the longwave ridge (fig. 4). Values of the FWI generally increase during the building half-cycle and decrease during the half-cycle of collapse. The times that "extreme" values of FWI were measured occur very close to the times of maximum ridging. The only exception is the "extreme" value centred on July 27th, which does not fit well with the ridge of July 31st.

In a practical sense, if the average period and lifetime of the longwave ridge cycle were known on June 14th, it would have been possible to predict the date of occurrence of "extreme" values of FWI in four cases out of five. The error in these cases would vary from 0 to 2 days. In the fifth case (the "extreme" FWI of July 11th), the prediction would have been five days too soon.

The forecast problem, and a very formidable one, is to recognize that a stable longwave ridge cycle has begun. While it is most probable that similar cycles have occurred in previous bad forest fire years, it would be too simplistic to believe that they have the same period and lifetime. Periodicity has been the goal at the end of the rainbow for many a meteorological researcher. Nevertheless, questions immediately arise concerning the feasibility of using such a regular variation as a forecasting device to predict times of high fire weather hazard.

5 Conclusions

(a) The longwave ridge oscillation of 1974 over northwestern Ontario showed a marked tendency towards a stable repeating periodicity of eleven days.
(b) The longwave ridge showed remarkable persistence, having a lifetime of 55 days.
(c) A close relationship existed between the time of occurrence of peaks in the longwave ridge oscillation and the times of high Fire Weather Index.
(d) A study of previous bad forest fire years is necessary in order to determine whether or not a common, predictable longwave ridge behaviour pattern exists.

References

ANDERSON, R., 1961: Wave motion in the upper westerlies. *Techniques for High-Level Analysis and Forecasting of Wind and Temperature Fields* WMO No. 106 TP 45, 29–42.

BJERKNES, J., 1957: Hovmöller diagram analysis Article II, *Large Scale Synoptic Processes*, Final report no. AF 19 (604)-1286, Dept. of Meteorology, UCLA. 27 pp.

FRANK, V.V., 1965: A method for the determination of relationships between the occurrence and spread of forest fires and the characteristics of the barometric field, *Current Problems in the Protection of Forests from Fires and Forest Fire Fighting*. Proceedings Leningrad Scientific Research Institute of Forestry. LESNAYA promyshlennost. Moskva, 1965, 38–52. (In Russian.)

HOVMÖLLER, E., 1949: The trough and ridge diagram. *Tellus*, 1, 62–66.

NOAR, P.F., 1973: Energy Dispersion and other Features of the Middle Latitude Circulation in the Australian Region. Meteorological Study no. 24, Australian Bureau of Meteorology, Department of Science.

BOOK REVIEW

ACTINOMETRY, ATMOSPHERIC OPTICS, OZONOMETRY. G.P. Gushchin, Editor. Keter Publishing House Jerusalem Ltd., Jerusalem, 1974, 201 pp, hardcover. Available in U.S. and Canada from International Scholarly Book Services, P.O. Box 4347, Portland, Oregon 97208, U.S. $16.00.

The "Trudy" series of the A.I. Voekov Main Geophysical Observatory (Leningrad) constitutes, in effect, an irregularly published scientific journal. This volume is a translation of No. 279, originally published in 1972, and consists of a collection of some twenty-two papers on various aspects of actinometry, atmospheric optics and atmospheric ozone. The papers range from a short evaluation of an electrolytic integrator used to measure daily totals of solar radiation in the USSR network to a lengthy discussion of ozone photochemistry. In addition, there are several papers on atmospheric transmission, both in the visible and the infrared; two papers on ozone and atmospheric dynamics; a catalogue of total ozone measurements made from USSR ships at various latitudes in the Indian Ocean during the decade 1961–1970; a description of a method for measurement of erythematogenic radiation; and others. Another paper, which is somewhat out of phase with current major concerns is entitled "Atmospheric ozone and its influence on the operation of supersonic transport".

While none of the papers is particularly outstanding, the book is one that probably should be borrowed from the library and looked through by those people who are expected, or who wish, to be expert in these particular fields. However, it can hardly be recommended as a worthwhile purchase to someone who is looking for an authoritative review or text in these fields.

C.L. Mateer
Atmospheric Environment Service
Toronto

MEMBERSHIP APPLICATION FORM

(Please write in Block Letters)

General or Student Member	SURNAME ....
	GIVEN NAMES ....
	PERMANENT ADDRESS ....
	....
	TITLE, RANK, DECORATIONS, DEGREES OR PROFESSIONAL QUALIFICATIONS ....
	OCCUPATION .... (for record purposes only; if student, indicate university and year studies will be completed)
Sustaining Member	NAME OR AGENCY ....
	BUSINESS ADDRESS ....
	....
Membership Status Required	Please enroll me as a .... member of the Canadian Meteorological Society effective January 1, 19......, to receive all publications issued by the Society from that date. I attach a cheque for $.............. payable to the *Canadian Meteorological Society*.

Signature of Applicant

Mail completed application forms to:
Corresponding Secretary
Canadian Meteorological Society
Dept. of Meteorology
McGill University
P.O. Box 6070
Montreal, P.Q. H3C 3G1

CMS dues for 1975.

General Member	$20.00
Student Member	$ 5.00
Sustaining Member	$60.00 (min.)

FORMULE D'ADHESION

(Lettres moulées, s.v.p.)

Membre ou Membre-etudiant

NOM ....

PRENOM(S) ....

ADRESSE ....

....

TITRE, RANG, DECORATIONS, DEGRES OU QUALIFICATION

PROFESSIONNELLES ....

....

OCCUPATION ....

(Pour registres seulement. L'étudiant doit inscrire le nom de son université et la date où il finira ses études)

Membre de soutien

NOM OU RAISON SOCIALE ....

ADRESSE ....

....

Type de Membre

J'aimerais devenir membre .... de la Société météorologique du Canada à compter du 1er janvier 19......., et recevoir toutes les publications de la Société par la suite. Vous trouverez ci-inclus un chèque de $.... .... libellé à *La Société météorologique du Canada.*

Signature du candidat

Envoyer cette formule d'adhésion au:
Secrétaire
Société météorologique du Canada
Département de Météorologie
McGill University, C.P. 6070
Montréal, Québec H3C 3G1

Cotisation annuelle, pour 1975.

Membre	$20.00
Membre étudiant	$ 5.00
Membre de soutien	$60.00 (min.)

INFORMATION FOR AUTHORS

Editorial policy. *Atmosphere* is a medium for the publication of the results of original research, survey articles, essays and book reviews in all fields of atmospheric science. It is published quarterly by the CMS with the aid of a grant from the Canadian Government. Articles may be in either English or French. Contributors need not be members of the CMS nor need they be Canadian; foreign contributions are welcomed. All contributions will be subject to a critical review before acceptance. Because of space limitations articles should not exceed 16 printed pages and preferably should be shorter.

Manuscripts should be submitted to: the Editor, *Atmosphere*, West Isle Office Tower, 5th Floor, 2121 Trans-Canada Highway, Dorval, Quebec H9P 1J3. Three copies should be submitted, typewritten with double spacing and wide margins. Heading and sub-headings should be clearly designated. A concise, relevant and substantial abstract is required.

Tables should be prepared on separate sheets, each with concise headings.

Figures should be provided in the form of three copies of an original which should be retained by the author for later revision if required. A list of legends should be typed separately. Labelling should be made in generous size so that characters after reduction are easy to read. Line drawings should be drafted with India ink at least twice the final size on white paper or tracing cloth. Photographs (halftones) should be glossy prints at least twice the final size.

Units. The International System (SI) of metric units is preferred. Units should be abbreviated only if accompanied by numerals, e.g., '10 m', but 'several metres.'

Footnotes to the text should be avoided.

Literature citations should be indicated in the text by author and date. The list of references should be arranged alphabetically by author, and chronologically for each author, if necessary.

RENSEIGNEMENTS POUR LES AUTEURS

Politique éditoriale. *Atmosphère* est un organe de publication de résultats de recherche originale d'articles sommaires, d'essais et de critiques dans n'importe lequel domaine des sciences de l'atmosphere. Il est publié par la SMC à l'aide d'une subvention accordée par le gouvernement canadien. Les articles peuvent être en anglais ou en français. Il n'est pas nécessaire que les auteurs soient membre de la SMC; les contributions étrangères sont bien-venues. A cause des limitations d'espace les articles ne doivent pas dépasser 16 pages dans le format final. Tout article sera soumis à un critique indépendant avant d'être accepté.

Les manuscrits doivent être envoyés à : le Rédacteur, *Atmosphère*, West Isle Office Tower, 5e étage, 2121 route Trans-canadienne, Dorval, Québec H9P 1J3. Ils doivent être soumis en trois exemplaires dactylographiés à double interlignes avec de larges marges. Les titres et sous-titres doivent être clairement indiqués. Chaque article doit comporter un résumé qui soit concis, pertinent et substantiel.

Les tableaux doivent être préparés et présentés séparément accompagnés d'un titre et d'un numéro explicatifs concis.

Les graphiques doivent être présentés en trois copies dont les originaux devraient être conservés par l'auteur au cas où ils seraient nécessaire de les reviser. Une liste des légendes des graphiques doit être dactylographiée séparément. L'étiquettage doit être de grand format de façon à ce qu'il soit facilement lisible après réduction du format. Le traçage des lignes doit s'effectuer au moyen d'encre de chine en doublant, au moins, le format final, le tout sur papier blanc ou sur papier à calquer et identifié adéquatement. Les photographies (demi-teintes) devraient être présentées sur épreuves glacées au double du format final.

Les unités. Le Système International (SI) d'unités métriques est préférable. Les unités devraient être abrégées seulement lorsqu'elles sont accompagnées de nombres, ex: "10m", mais "plusieurs mètres".

Les notes de renvoie au texte doivent être évitées.

Les citations littéraires doivent être indiquées dans le texte selon l'auteur et la date. La liste des références doit être présentée dans l'ordre alphabétique, par auteur et, si nécessaire, dans l'ordre chronologique pour chaque auteur.

The Canadian Meteorological Society / La Société Météorologique du Canada

The Canadian Meteorological Society came into being on January 1, 1967, replacing the Canadian Branch of the Royal Meteorological Society, which had been established in 1940. The Society exists for the advancement of Meteorology, and membership is open to persons and organizations having an interest in Meteorology. At nine local centres of the Society, meetings are held on subjects of meteorological interest. *Atmosphere* as the scientific journal of the CMS is distributed free to all members. Each spring an annual congress is convened to serve as the National Meteorological Congress.

Correspondence regarding Society affairs should be directed to the Corresponding Secretary, Canadian Meteorological Society, c/o Dept. of Meteorology, McGill University, P.O. Box 6070, Montreal, P.Q. H3C 3G1

There are three types of membership – Member, Student Member and Sustaining Member. For 1975 the dues are $20.00, $5.00 and $60.00 (min.), respectively. The annual Institutional subscription rate for *Atmosphere* is $15.00.

Correspondence relating to CMS membership or to institutional subscriptions should be directed to the University of Toronto Press, Journals Department, 5201 Dufferin St., Downsview, Ontario, Canada, M3H 5T8. Cheques should be made payable to the University of Toronto Press.

La Société météorologique du Canada a été fondée le 1er janvier 1967, en replacement de la Division canadienne de la Société royale de météorologie, établie en 1940. Cette société existe pour le progrès de la météorologie et toute personne ou organisation qui s'intéresse à la météorologie peut en faire partie. Aux neuf centres locaux de la Société, on peut y faire des conférences sur divers sujets d'intérêt météorologique. *Atmosphere*, la revue scientifique de la SMC, est distribuée gratuitement à tous les membres. À chaque printemps, la Société organise un congrès qui sert de Congrès national de météorologie.

Toute correspondance concernant les activités de la Société devrait être adressée au Secrétaire-correspondant, Société météorologique du Canada, Département de Météorologie, l'Université McGill, C.P. 6070, Montréal, P.Q. H3C 3G1

Il y a trois types de membres: Membre, Membre-étudiant, et Membre de soutien. La cotisation est, pour 1975, de $20.00, $5.00 et $60.00 (min.) respectivement. Les Institutions peuvent souscrire à *Atmosphère* au coût de $15.00 par année.

La correspondance concernant les souscriptions au SMC ou les souscriptions des institutions doit être envoyée aux Presses de l'Université de Toronto, Département des périodiques, 5201 Dufferin St., Downsview, Ontario, Canada, M3H 5T8. Les chèques doivent être payables aux Presses de l'Université de Toronto.